

Derivation of a Second-Order Switching Surface in the Boundary Control of Buck Converters

Kelvin K. S. Leung, *Student Member, IEEE*, and Henry S. H. Chung, *Senior Member, IEEE*

Abstract—A second-order switching surface in the boundary control of buck converters is derived in this letter. The formulated switching surface can make the overall converter exhibit better steady-state and transient behaviors than the one with a first-order switching surface. The switching surface is derived by estimating the state trajectory movement after a switching action, resulting in a high state trajectory velocity along the switching surface. This phenomenon accelerates the trajectory moving toward the target operating point. The proposed control scheme has been successfully applied to a 120-W buck converter. The large-signal performance and a comparison with the first-order switching surface have been studied.

Index Terms—Boundary control, dc/dc conversion, large-signal stability.

I. INTRODUCTION

SWITCHING converters are an important class of systems that operate by variable structure control. Boundary control is a geometrically-based control method suitable for those switching converters having time-varying circuit topology. Based on the large-signal trajectories of the converter on the state plane, a switching surface is defined to dictate the switching actions. An ideal switching surface can achieve global stability, good large-signal operation, and fast dynamics [1]. Detailed investigations into the modeling, design, and analysis of the boundary control with a first-order switching surface are carried out in [1]–[3].

Among various boundary control methods with first-order switching surfaces, sliding-mode control, and hysteresis control are widely used in power converters [4]–[7]. Although these methods generally provide good large-signal performance and stability, the transient dynamics is not optimized. Much research has extended these concepts, such as adaptive-hysteresis control in [8], [9], to enhance the dynamics. However, many of the methods are applicable only for dc/dc converters operating in continuous conduction mode. When a converter is operated in the discontinuous conduction mode, an additional boundary due to the zero inductor current is created. An unstable combination may emerge [2]. Moreover, with the presence of the hysteresis band, the output will even contain a steady-state error.

A second-order switching surface in the boundary control of buck converters is presented in this letter. The proposed

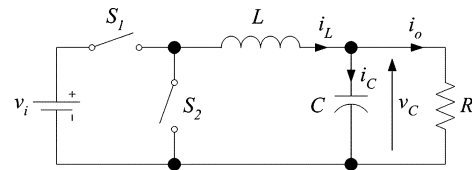


Fig. 1. Circuit schematics of buck converter.

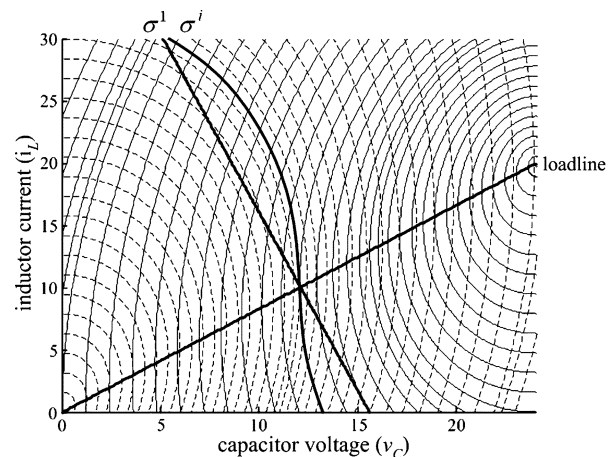


Fig. 2. State trajectory families of buck converter with σ^1 and σ^i . (Solid line: on-trajectories, dotted line: off-trajectories.)

switching surface enhances the tangential velocity of the trajectories along the switching surface, so that the converter exhibits better transient behaviors than the one with the first-order switching surface. Instead of guiding the state trajectory movement as in the first-order switching surface, the proposed surface is derived from the natural movement of the state trajectory after a switching action. The proposed control scheme has been successfully applied to a 120-W buck converter.

II. FIRST- AND SECOND-ORDER SWITCHING SURFACES

The buck converter shown in Fig. 1 can be expressed by the state-space equation of

$$\dot{x} = A_0x + B_0u + (A_1x + B_1u)q_1 + (A_2x + B_2u)q_2 \quad (1)$$

where A_i and B_i are constant matrix and q_i represents the state of the switch S_i . S_i is on if $q_i = 1$, and is off if $q_i = 0$.

A family of the on- and off-state trajectories, as well as the load line, is shown in Fig. 2. The trajectories are obtained by solving (1) with different initial conditions. The component values used in the analysis are tabulated in Table I. The on-state trajectory is obtained by setting $\{q_1, q_2\} = \{1, 0\}$, while the off-state trajectory is obtained by setting $\{q_1, q_2\} = \{0, 1\}$.

Manuscript received March 11, 2004; revised July 14, 2004. This work was supported by a Strategic Research Grant from the City University of Hong Kong under Project 7001595. Recommended by Associate Editor J. Sun.

The authors are with the Department of Electronic Engineering, City University of Hong Kong, Kowloon, Hong Kong (e-mail: eeshc@cityu.edu.hk).

Digital Object Identifier 10.1109/LPEL.2004.834796

TABLE I
COMPONENT VALUES OF THE BUCK CONVERTER

Parameter	Value
v_i	24V
v_{ref}	12V
L	100 μ H
C	400 μ F
R	1.2 Ω
c_1	0.2702
$\{k_1, k_2\}$	$\{0.0104, 0.0104\}$

As discussed in [1], the tangential component of the state-trajectory velocity on the switching surface determines the rate at which successor points approach or recede from the target operating point. An ideal switching surface σ^i that gives fast dynamics should be on the only trajectory passing through the target operating point. Once the converter state reaches the surface, it will theoretically attract to target operating point in one successive switching cycle. As shown in Fig. 2, the surface of σ^i above the load line should be along the only off-state trajectory that passes the target operating point and the surface of σ^i below the load line should be along the only on-state trajectory that passes the target operating point. The converter will follow the off-state trajectory when its state is at the right hand side of σ^i and will follow the on-state trajectory when its state is at the left hand side of σ^i .

A typical first-order switching surface σ^1 is shown in Fig. 2 and can be written in the following single-reference form:

$$\begin{aligned}\sigma^1(i_L, v_C) &= c_1 i_C + (v_C - v_{ref}) \\ &= c_1 \left(i_L - \frac{v_C}{R} \right) + (v_C - v_{ref})\end{aligned}\quad (2)$$

where i_C and v_C are the capacitor current and voltage, respectively, i_L is the inductor current, c_1 is the gain, R is the load resistance, and v_{ref} is the desired output voltage.

Thus, the tangential state-trajectory velocity on σ^1 is nonoptimal such that the transient dynamics may take several switching cycles. A second-order surface σ^2 , which is near to the ideal surface around the operating point, is derived in the following. The concept is based on estimating the state trajectory after a hypothesized switching action. If the output ripple voltage is much smaller than the average output voltage at the steady state, the output current i_o is relatively constant. Since $i_L = i_C + i_o$, the change of i_L , Δi_L , equals the change of i_C , Δi_C . Fig. 3 shows the typical waveforms of v_C and i_C . v_C varies between a maximum value of $v_{C,max}$ and a minimum value of $v_{C,min}$. The state of S is determined by predicting the area under i_C with a hypothesized switching action until $i_C = 0$, and then comparing the area with a fixed ratio of the output error at that instant. Criteria for switching S_1 are given below.

A. Criteria for Switching Off S_1

As shown in Fig. 3, S_1 is originally in the on state and is switched off at the hypothesized time instant t_1 . The objective is to determine t_1 , so that v_C is equal to $v_{C,max}$ at t_2 (at which

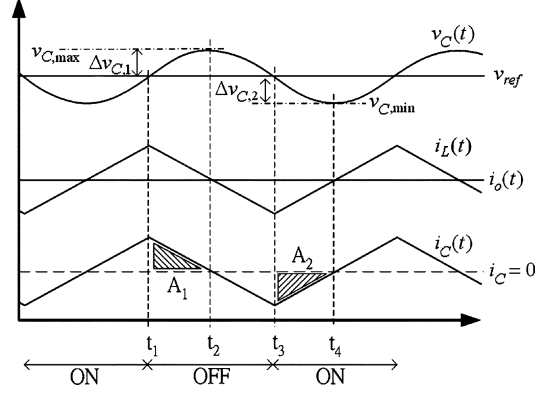


Fig. 3. Typical waveforms of v_C , i_L , i_C , and i_o of buck converter.

$i_C = 0$). The shaded area A_1 under i_C is integrated from t_1 to t_2 . Thus

$$\Delta v_{C,1} = v_{C,max} - v_C(t_1) = \frac{1}{C} \int_{t_1}^{t_2} i_C dt. \quad (3)$$

Again, A_1 is approximated by a triangle. It can be shown that

$$\int_{t_1}^{t_2} i_C dt \cong \frac{1}{2} \frac{Li_C^2(t_1)}{v_C(t_1)}. \quad (4)$$

[see derivations of (3) and (4) in the Appendix.] In order to ensure that v_C will not go above $v_{C,max}$, S_1 should be switched off when

$$v_C(t_1) \geq v_{C,max} - \frac{1}{2} \frac{Li_C^2(t_1)}{Cv_C(t_1)} = v_{C,max} - k_1(v_C)i_C^2(t_1) \quad (5)$$

and

$$i_C(t_1) > 0. \quad (6)$$

B. Criteria for Switching on S_1

As shown in Fig. 3, S_1 is originally off and is switched on at the hypothesized time instant t_3 . The objective is to determine t_3 , so that v_C is equal to $v_{C,min}$ at t_4 (at which $i_C = 0$). The shaded area A_2 under i_C is integrated from t_3 to t_4 . Thus

$$\Delta v_{C,2} = v_{C,min} - v_C(t_3) = \frac{1}{C} \int_{t_3}^{t_4} i_C dt. \quad (7)$$

If A_2 is approximated by a triangle, it can be shown that

$$\int_{t_3}^{t_4} i_C dt \cong -\frac{1}{2} \frac{Li_C^2(t_3)}{[v_i(t_3) - v_C(t_3)]}. \quad (8)$$

[Derivations of (7) and (8) can be found in the Appendix.] In order to ensure that v_C will not go below $v_{C,min}$, S_1 should be switched on when

$$\begin{aligned}v_C(t_3) &\leq v_{C,min} + \frac{1}{2} \frac{Li_C^2(t_3)}{C[v_i(t_3) - v_C(t_3)]} \\ &= v_{C,min} + k_2(v_i, v_C)i_C^2(t_3)\end{aligned}\quad (9)$$

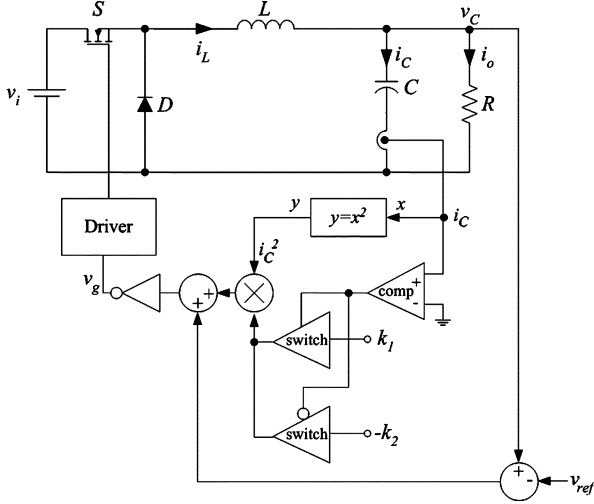


Fig. 4. Implementation of the controller.

and

$$i_C(t_3) < 0. \quad (10)$$

For simplicity, k_1 and k_2 are obtained by using the nominal values of v_i and v_C . Based on (5), (6), (9), (10), and $v_{C,\min} = v_{C,\max} = v_{\text{ref}}$, the following σ^2 can be concluded:

$$\sigma^2(i_L, v_C) = \begin{cases} k_1 \left(i_L - \frac{v_C}{R}\right)^2 + (v_C - v_{\text{ref}}), & \left(i_L - \frac{v_C}{R}\right) > 0 \\ -k_2 \left(i_L - \frac{v_C}{R}\right)^2 + (v_C - v_{\text{ref}}), & \left(i_L - \frac{v_C}{R}\right) < 0. \end{cases} \quad (11)$$

The equation can further be written into a single expression of

$$\sigma^2(i_L, v_C) = c_2 \left(i_L - \frac{v_C}{R}\right)^2 + (v_C - v_{\text{ref}}) \quad (12)$$

where $c_2 = (1/2)k_1(1 + \text{sgn}(i_L - (v_C/R))) - (1/2)k_2(1 - \text{sgn}(i_L - (v_C/R)))$.

Comparing (12) with σ^1 in (2), σ^2 consists of a second-order term. σ^2 is close to σ^i near the operating point. However, discrepancies occur when the state is far from the operating point because of the approximations in (4) and (8). Implementation of the controller is shown in Fig. 4.

III. LARGE-SIGNAL STABILITY

Points along $\sigma = 0$ can be classified into refractive, reflective, and rejective modes. The dynamics of the system will be exhibited differently in these regions [1]. For σ^2 , the transition boundary is obtained by differentiating (12) so that

$$\left. \frac{di_L}{dv_C} \right|_{\text{on,off}} = \frac{1}{R} + \frac{1}{2} \frac{i_L - \frac{v_C}{R}}{v_C - v_{\text{ref}}}. \quad (13)$$

The expression at the left-hand side can be derived by using the state equations in (1). Based on (13), the transition boundary with S_1 on is

$$\frac{C}{L} \left(\frac{v_i - v_C}{i_L - \frac{v_C}{R}} \right) = \frac{1}{R} + \frac{1}{2} \frac{i_L - \frac{v_C}{R}}{v_C - v_{\text{ref}}} \quad (14)$$

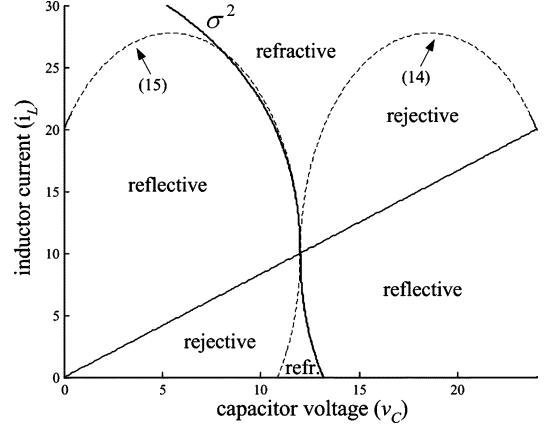


Fig. 5. Transition boundaries.

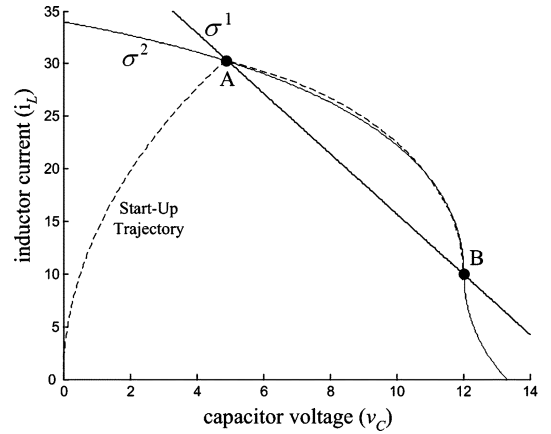


Fig. 6. Startup transient response and the first- and second-order switching surface. (Dotted line: startup trajectory of buck converter.)

and the transition boundary with S_1 off is

$$-\frac{C}{L} \left(\frac{v_C}{i_L - \frac{v_C}{R}} \right) = \frac{1}{R} + \frac{1}{2} \frac{i_L - \frac{v_C}{R}}{v_C - v_{\text{ref}}}. \quad (15)$$

Fig. 5 combines the transition boundaries of (14) and (15). When the state is near the operating point, σ^2 is almost along the boundary between the reflective and refractive regions. The state of the converter will move along the switching surface in the reflective region, which is similar to the sliding-mode control. Once the state enters into the boundary between the reflective and refractive regions, the system will go to the target operating point in the next switching action.

IV. EXPERIMENTAL VERIFICATIONS

A buck converter with the tabulated component values in Table I is studied. Fig. 6 shows the startup trajectory, together with σ^1 and σ^2 . σ^1 is formulated by having the same startup transients with σ^2 (i.e., σ^1 and σ^2 intercept at points "A" and "B" in Fig. 6). The hysteresis band in σ^1 is adjusted to give the same output ripple at the rated power as with σ^2 . Fig. 7 shows a comparison of the simulated transient responses when R is changed from 2.4Ω (60 W) to 1.2Ω (120 W), and *vice versa*, with σ^1 and σ^2 , respectively. The converter with σ^2 achieves a faster transient response than with σ^1 . Fig. 8 shows the transient

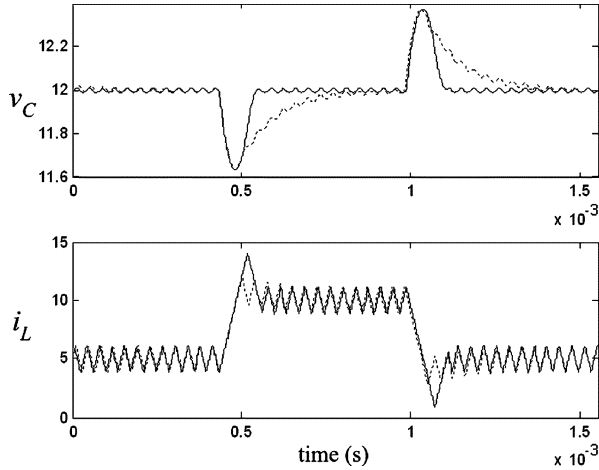


Fig. 7. Transient response of R from 2.4Ω to 1.2Ω and vice versa. (Solid line: σ^2 , dotted line: σ^1).

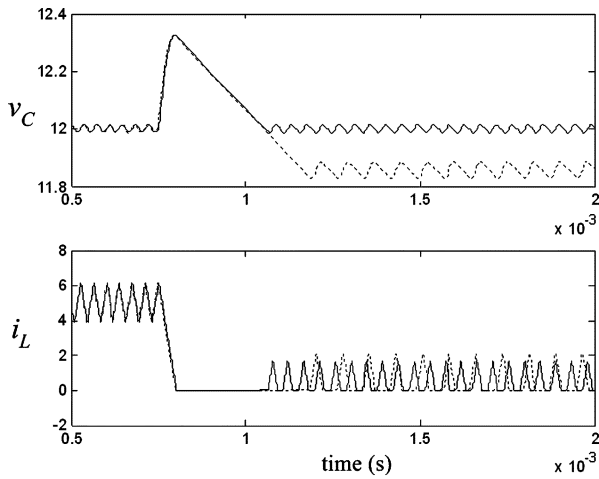


Fig. 8. Transient response of R from 2.4 to 24Ω . (Solid line: σ^2 , dotted line: σ^1).

responses when R is changed from 2.4Ω (60 W) to 24Ω (6 W), in which the converter is operated in discontinuous conduction mode with $R = 24 \Omega$. Results show that a steady-state error exists with σ^1 and is zero with σ^2 . The additional boundary due to the zero inductor current causes a shift of the effective output voltage reference. Figs. 9 and 10 show the experimental results corresponding to the above testing conditions and are in close agreement with the theoretical predictions. It can be observed that the converter can go to the steady state in two switching actions.

V. CONCLUSION

A boundary control using the second-order switching surfaces in buck converters has been proposed. Large-signal stability and the transient response are investigated. Results show that a second-order switching surface can achieve near-optimum large-signal responses. Future publications will show how this concept applies to the discontinuous mode.

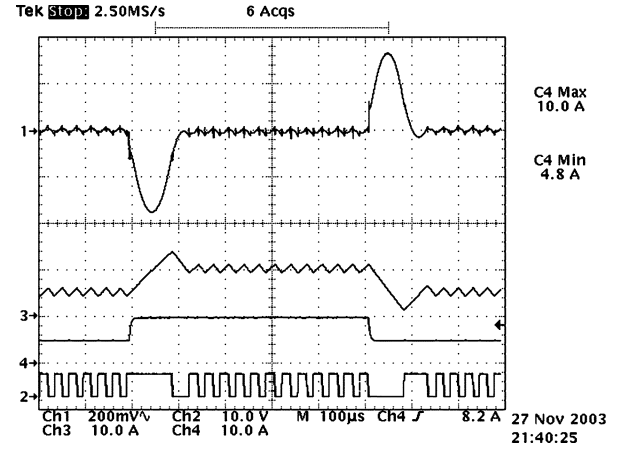


Fig. 9. Transient response of buck converter using second-order switching surface control. Load change from 5 A (2.4Ω) to 10 A (1.2Ω) and vice versa. [Ch1: v_C (200 mV/div), Ch2: v_g (10 V/div), Ch3: i_L (10 A/div), Ch4: i_o (10 A/div)] (Timebase: $100 \mu\text{s/div}$.)

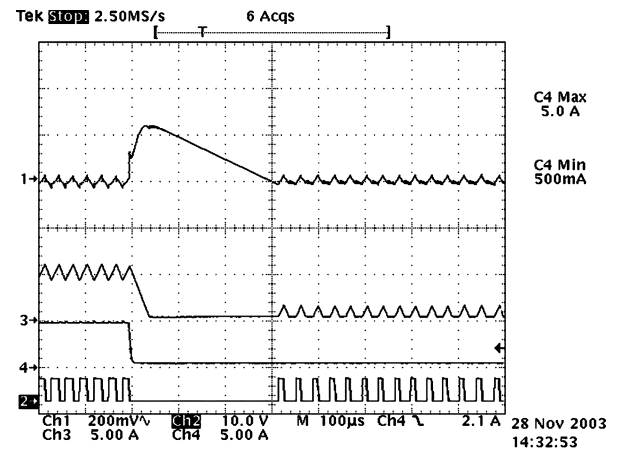


Fig. 10. Transient response of buck converter using second-order switching surface control. Load change from 5 A (2.4Ω) to 0.5 A (24Ω). [Ch1: v_C (200 mV/div), Ch2: v_g (10 V/div), Ch3: i_L (5 A/div), Ch4: i_o (5 A/div)] (Timebase: $100 \mu\text{s/div}$.)

APPENDIX

a) Proof of (3) and (4): During the off-state

$$i_C = C \frac{dv_C}{dt} \quad (\text{A1})$$

$$-v_C = L \frac{di_L}{dt}. \quad (\text{A2})$$

By using $i_L = i_C + i_o$ and assuming i_o to be constant

$$\begin{aligned} \frac{di_C}{dt} &= \frac{di_L}{dt} \approx -\frac{v_C(t_1)}{L} \\ dt &= -\frac{L}{v_C(t_1)} di_C. \end{aligned} \quad (\text{A3})$$

Based on (A1)

$$\int_{t_1}^{t_2} dv_C = \frac{1}{C} \int_{t_1}^{t_2} i_C dt. \quad (\text{A4})$$

Thus, (3) can be derived from (A4) such that

$$\Delta v_{C,1} = v_C(t_2) - v_C(t_1) = v_{C,\max} - v_C(t_1) = \frac{1}{C} \int_{t_1}^{t_2} i_C dt. \quad (\text{A5})$$

By substituting (A3) and $i_C(t_2) = 0$ into $(1/C) \int_{t_1}^{t_2} i_C dt$, (4) can be expressed as

$$\begin{aligned} \int_{t_1}^{t_2} i_C dt &= \int_{i_C(t_1)}^{i_C(t_2)} i_C \cdot \left(-\frac{L}{v_C(t_1)} \right) di_C \\ \int_{t_1}^{t_2} i_C dt &= -\frac{L}{v_C(t_1)} \int_{i_C(t_1)}^0 i_C di_C = \frac{1}{2} \frac{Li_C^2(t_1)}{v_C(t_1)}. \end{aligned} \quad (\text{A6})$$

b) *Proof of (7) and (8):* During the on-state

$$i_C = C \frac{dv_C}{dt} \quad (\text{A7})$$

$$v_i - v_C = L \frac{di_L}{dt}. \quad (\text{A8})$$

By using $i_L = i_C + i_o$ and assuming i_o to be constant

$$\begin{aligned} \frac{di_C}{dt} &= \frac{di_L}{dt} \cong \frac{v_i(t_3) - v_C(t_3)}{L} \\ dt &= \frac{L}{v_i(t_3) - v_C(t_3)} di_C. \end{aligned} \quad (\text{A9})$$

Based on (A7)

$$\int_{t_3}^{t_4} dv_C = \frac{1}{C} \int_{t_3}^{t_4} i_C dt. \quad (\text{A10})$$

Thus, (7) can be derived from (A.10)

$$\Delta v_{C,2} = v_C(t_4) - v_C(t_3) = v_{C,\min} - v_C(t_3) = \frac{1}{C} \int_{t_3}^{t_4} i_C dt. \quad (\text{A11})$$

By substituting (A9) and $i_C(t_4) = 0$ into $(1/C) \int_{t_3}^{t_4} i_C dt$, (8) can be expressed as

$$\begin{aligned} \int_{t_3}^{t_4} i_C dt &= \int_{i_C(t_3)}^{i_C(t_4)} i_C \cdot \left(\frac{L}{v_i(t_3) - v_C(t_3)} \right) di_C \\ \int_{t_3}^{t_4} i_C dt &= \frac{L}{v_i(t_3) - v_C(t_3)} \int_{i_C(t_3)}^0 i_C di_C \\ &= -\frac{1}{2} \frac{Li_C^2(t_3)}{[v_i(t_3) - v_C(t_3)]}. \end{aligned} \quad (\text{A12})$$

REFERENCES

- [1] P. T. Krein, *Nonlinear Phenomena in Power Electronics: Attractors, Bifurcation, Chaos, and Nonlinear Control*. Piscataway, NJ: IEEE Press, 2001, ch. 8.
- [2] R. Munzert and P. T. Krein, "Issues in boundary control," in *Rec., IEEE Power Electronics Specialists Conf.*, 1996, pp. 810–816.
- [3] M. Greuel, R. Muyschondt, and P. T. Krein, "Design approaches to boundary controllers," in *Rec., IEEE Power Electronics Specialists Conf.*, 1997, pp. 672–678.
- [4] M. Carpita and M. Marchesoni, "Experimental study of a power conditioning system using sliding mode control," *IEEE Trans. Power Electron.*, vol. 11, pp. 731–742, Sept. 1996.
- [5] B. J. Cardoso, A. F. Moreira, B. R. Menezes, and P. C. Cortizo, "Analysis of switching frequency reduction methods applied to sliding-mode controlled DC-DC converters," in *Rec., IEEE Applied Power Electronics Conf. Exposition*, 1992, pp. 403–410.
- [6] C. H. Tso and J. C. Wu, "A ripple control buck regulator with fixed output frequency," *IEEE Power Electron. Lett.*, vol. 1, pp. 61–63, Sept. 2003.
- [7] R. Miftakhutdinov, "Analysis of synchronous buck converter with hysteretic controller at high slew-rate load current transients," in *Rec., High Frequency Power Conversion Conf.*, 1999, pp. 55–69.
- [8] V. M. Nguyen and C. Q. Lee, "Tracking control of buck converter using sliding-mode with adaptive hysteresis," in *Rec., IEEE Power Electronics Specialists Conf.*, 1995, pp. 1086–1093.
- [9] A. S. Kislovski, R. Redl, and N. O. Sokal, *Dynamic Analysis of Switching-Mode DC-DC Converters*. New York: Van Nostrand, 1991.